



CHORUS

This is the accepted manuscript made available via CHORUS. The article has been published as:

Electrically tunable spin polarization of chiral edge modes in a quantum anomalous Hall insulator

Rui-Xing Zhang, Hsiu-Chuan Hsu, and Chao-Xing Liu

Phys. Rev. B **93**, 235315 — Published 27 June 2016

DOI: [10.1103/PhysRevB.93.235315](https://doi.org/10.1103/PhysRevB.93.235315)

Electrically tunable spin polarization of chiral edge modes in a quantum anomalous Hall insulator

Rui-Xing Zhang,¹ Hsiu-Chuan Hsu,¹ and Chao-Xing Liu^{1,*}

¹*Department of Physics, The Pennsylvania State University, University Park, Pennsylvania 16802*

(Dated: June 6, 2016)

In the quantum anomalous Hall effect, chiral edge modes are expected to conduct spin polarized current without dissipation and thus hold great promise for future electronics and spintronics with low energy consumption. However, spin polarization of chiral edge modes has never been established in experiments. In this work, we theoretically study spin polarization of chiral edge modes in the quantum anomalous Hall effect, based on both the effective model and more realistic tight-binding model constructed from the first principles calculations. We find that spin polarization can be manipulated by tuning either a local gate voltage or the Fermi energy. We also propose to extract spin information of chiral edge modes by contacting the quantum anomalous Hall insulator to a ferromagnetic (FM) lead. The establishment of spin polarization of chiral edge modes, as well as the manipulation and detection in a fully electrical manner, will pave the way to the applications of the quantum anomalous Hall effect in spintronics.

PACS numbers: 73.20.-r, 72.25.-b, 85.75.-d

Introduction - For a two dimensional electron gas under a strong magnetic field, Landau levels are formed and drive the system into a state characterized by the zero longitudinal resistance and the quantized Hall conductance with an integer value of $\frac{e^2}{h}$. This phenomenon is known as the quantum Hall (QH) effect, which was discovered by Von. Klitzing in 1980¹. Recently, it was theoretically predicted²⁻⁴ that this type of quantization in the Hall conductance can also be realized in magnetic insulating materials at a zero external magnetic field. This phenomenon, dubbed as the “quantum anomalous Hall (QAH) effect”, was soon observed experimentally in magnetically doped topological insulators (TIs), the Cr or V doped (Bi,Sb)₂Te₃ films⁵⁻⁹. The physical origin of the QAH effect is spin-orbit coupling and exchange coupling between magnetic moments and electron spins in magnetic materials, rather than magnetic fields and the associated Landau levels². The experimental observation of the exact quantization of Hall conductance and negligible longitudinal resistance confirm the dissipationless nature of transport for the QAH effect^{8,9} and the mapping of global phase diagram establishes the topological equivalence between the QH effect and the QAH effect^{7,10}.

Similar to the case of the QH effect, dissipationless currents in the QAH insulators are carried by one dimensional (1D) chiral edge modes (CEMs), which propagate along one direction at the edge of the system and are robust against disorder scatterings. CEMs are believed to hold great promise for the potential applications in electronics and spintronics with low power consumption¹¹. For any spintronic application, it is required for CEMs to carry spin polarization (SP). Naively, one may expect that SP of CEMs should exist and follows bulk magnetization, but this issue has seldom been studied theoretically. In Ref.¹², SP of CEMs was studied in the context of a two band model, which is more relevant to cold atom systems. For condensed matter systems, it is more complicated since spin and orbital are mixed with each other

due to spin-orbit coupling¹³.

In this letter, we investigate SP of CEMs of the QAH effect in magnetically doped (Bi,Sb)₂Te₃. Surprisingly, we find that SP of CEMs though exists but does not follow bulk magnetization, and sensitively depends on the boundary conditions. In particular, we find that the direction of SP of CEMs can be manipulated by a local gate voltage, thus opening the possibility of controlling SP of CEMs in a fully electrical manner. We provide a simple physical picture of SP of CEMs based on the effective four-band model and further study its behavior in the more realistic calculations based on the tight-binding model constructed by the Wannier function method of the first principles calculations^{14,15}. We propose the spin valve effect¹⁶ of CEMs in a standard experimental setup of the Hall measurement with ferromagnetic (FM) leads to extract spin information of CEMs.

Spin polarization of chiral edge modes - To study SP of CEMs in a QAH insulator, we first consider an effective four band model for magnetically doped (Bi,Sb)₂Te₃ films⁴. The low energy physics of this system is dominated by two surface states from top and bottom surfaces, which hybridize with each other to open a gap due to the finite size effect. Meanwhile, the exchange coupling of electron spin arises from the doping of magnetic atoms. Thus, the effective Hamiltonian H_{eff} is given by

$$H_{eff} = v\tau_z \otimes (k_y\sigma_x - k_x\sigma_y) + m(\mathbf{k})\tau_x \otimes \sigma_0 + \mathbf{M} \cdot \tau_0 \otimes \vec{\sigma} + V(x, y)\tau_z \otimes \sigma_0 + A(k)\tau_0 \otimes \sigma_0 + h(k_+^3 + k_-^3)\tau_0 \otimes \sigma_z, \quad (1)$$

where $\sigma_{x,y,z}$ and $\tau_{x,y,z}$ matrices are Pauli matrices of spin and layer (top or bottom) degree of freedom, and $\sigma_0 = \tau_0 = I_{2 \times 2}$. $m(\mathbf{k}) = m_0 + m_2(k_x^2 + k_y^2)$ gives hybridization between the top and bottom surface states. The \mathbf{M} term describes exchange coupling between electron spin and magnetization of magnetic doping. We only consider the out-of-plane magnetization M_z . $A(k) = A_0 + A_1(k_x^2 + k_y^2)$

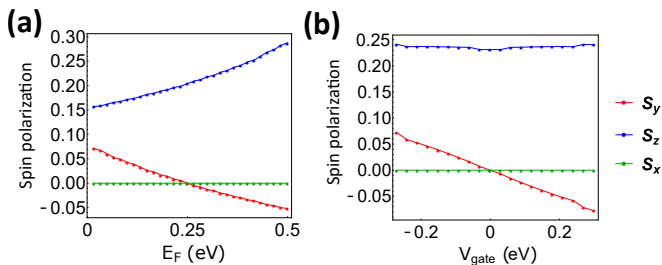


FIG. 1. Spin polarization $S_{x,y,z}$ of chiral edge state in our effective model is plotted at fixed local gate voltage ($V = 0.1$ eV) in (a), and at fixed Fermi energy ($E_F = 0.35$ eV) in (b).

is a higher order correction of the surface states and h is defined as the strength of hexagon warping effect^{17,18}. The V term denotes the asymmetric potential between the top and bottom layers which has spatial dependence and can be induced by a global or local gate voltage.

The edge spectrum of our effective model, as well as the corresponding SP, can be evaluated with the help of the iterative Green's function method^{19,20}. We consider a semi-infinite system with the x direction still translationally invariant and one edge parallel to x direction (x-edge). The following set of parameters, $v = 1$, $M_z = 0.5$, $m_0 = 0.1$, $m_2 = 0.25$, $A_0 = 0.15$, $A_1 = 0.05$, $h = 0.1$, is chosen to keep the system in the QAH regime. The local Green's function $G(k_x, \omega)$ on the x-edge can be evaluated iteratively. The total local density of states (DOS) and the spin DOS along the i th direction ($i = x, y, z$) are defined as $\rho_0 = -\frac{1}{\pi}\text{Im}[\text{tr}(G)]$ and $\rho_{\sigma_i} = -\frac{1}{\pi}\text{Im}[\text{tr}(G\sigma_i)]$, respectively. As shown in the Supplementary Materials¹³, the CEM can be easily identified from the peak of local DOS ρ_0 on the x-edge. The corresponding SP S_i along the i th direction ($i = x, y, z$) for the CEM is normalized by the total DOS as $S_i = \rho_{\sigma_i}/\rho_0$. In Fig. 1 (a) and (b), the SP of the CEMs is plotted for all three spin components with different local gate voltages and chemical potentials. Let us take the lattice constant to be unity and label the lattice site with an integer index $n \geq 1$, with $(n - 1)$ being the distance between the n th lattice site and the boundary. Here the local gate voltage V is added only on all $n = 1$ lattice sites, which leaves the bulk states unchanged. We find that for a zero gate voltage ($V = 0$), only the z component (S_z) SP of CEMs is non-zero. If we apply a local gate voltage, SP becomes non-zero for both the y and z direction, but still keeps zero for the x direction. Therefore, SP of CEMs can exist within the y - z plane and can be controlled by a local gate voltage. It is also interesting to notice that the local gate voltage mainly controls the amplitude of S_y , but barely change that of S_z (see Fig. 1(b))¹³. The chemical potential can also tune the magnitude of S_z (both S_y and S_z) at a zero (finite) local gate voltage, as shown in Fig. 1 (a). Therefore, our effective model (Eq. 1) suggests that SP of CEMs can be manipulated by either applying a local gate voltage or tuning the chemical potential.

Next we provide an analytical solution of the eigen

wave function for the Hamiltonian (Eq. 1) with $V = A_0 = A_1 = h = 0$ to understand the electrical tunability of SP of CEMs. Assume $m_{0,2} > 0$, the system will enter QAHE regime when $|M_z| > m_0$. The zero mode of the Hamiltonian H_{eff} localizing on the edge can be solved exactly¹³ as

$$\Psi(y) = C(e^{-\lambda_+^- y} - e^{-\lambda_-^- y})[|t\rangle \otimes (|\uparrow_y\rangle) + |b\rangle \otimes (|\downarrow_y\rangle)], \quad (2)$$

where C is a normalization factor and $\lambda_{\pm} = \frac{1}{2m_2}(v \pm \sqrt{v^2 + 4m_2(m_0 - M_z)})$. Here $|\uparrow_y$ ($|\downarrow_y$) denote spin up (down) state along the y direction, and $|t(b)\rangle$ denotes the contribution from the top (bottom) layer of thin films. The wave function (2) of CEMs consists of two parts: one part on the top surface with SP along the $+y$ direction and the other on the bottom surface with SP along the $-y$ direction. Thus, the SP is locked to the layer (top or bottom) for the CEMs. A local gate voltage can push the wave functions of CEMs into one layer, thus leading to the change of SP.

The above analysis of SP of CEMs is based on the effective four-band model (Eq. 1) and one may ask if these results still hold for a realistic system, such as Cr or V doped $(\text{Bi,Sb})_2\text{Te}_3$. To answer this question, we carry out explicit calculations for a magnetically doped Sb_2Te_3 thin film system with the realistic tight-binding model constructed from the maximal localized Wannier function (MLWF) method^{14,15} based on the first principles calculations, which has been successfully applied to the quantitative study of the QAH effect in magnetically doped $(\text{Bi,Sb})_2\text{Te}_3$ ^{21,22}. The exchange coupling between electron spin and magnetization is included in the tight-binding model in the mean field approximation $H_{\text{ex}} = \lambda_{\text{Sb}}\sigma_z^{\text{Sb}} + \lambda_{\text{Te}}\sigma_z^{\text{Te}}$. Here we consider only the contribution from out-of-plane magnetization and $\sigma_z^{\text{Sb(Te)}}$ is the z directional spin operator for Sb (Te) atoms. In our calculation, we consider a film with two quintuple layers and choose the exchange coupling strength to be $\lambda_{\text{Sb}} = 0.4$ eV and $\lambda_{\text{Te}} = 0.0$ eV, which is strong enough to drive the system into the QAH phase. The edge dispersion is also calculated with the iterative Green function method in a semi-infinite configuration along (100) direction, as shown in Fig. 2 (a). For edge modes, we find three left movers (the modes I, II and IV) and two right movers (the modes III and V), suggesting that one chiral edge mode (left mover) and the other two trivial 1D edge modes (or non-chiral edge modes)²¹. Since the mode IV is directly connected to V, these two modes must be trivial 1D edge modes and thus we focus on the modes I, II and III below. The influence of the local gate voltage ($V = 0.1$ eV) is shown in Fig. 2 (b), from which one can see that the number of left and right movers is unchanged, but their energy dispersions are shifted.

After obtaining the edge state Green function, it is straightforward to calculate the corresponding SP vector \mathbf{S} . First of all, S_x is vanishingly small compared to other spin components. This confirms the results from the effective four band model. Thus, \mathbf{S} only appears in the y - z

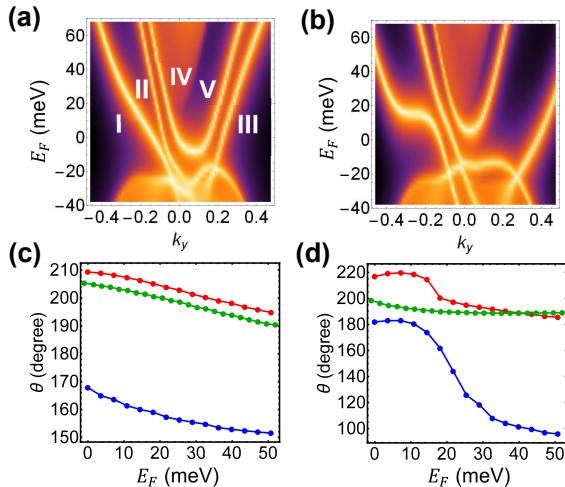


FIG. 2. Edge spectrum and edge state SP angle θ for magnetically doped Sb_2Te_3 QAH systems are plotted with: (1) $V = 0$ eV in (a) and (c). (2) $V = 0.1$ eV in (b) and (d). In (c) and (d), SP angle of edge mode I, II and III are plotted in red, blue and green.

plane and can be characterized by its magnitude $|S|$ and a polarization angle θ relative to $+z$ axis. For S_y , we notice that it vanishes at $V = 0$ for the effective four band model, while it is non-zero in the realistic tight-binding model. This difference is because of the out-of-plane mirror symmetry in our four band model, which is absent in realistic crystals. Therefore, both S_y and S_z are non-zero even at $V = 0$ in realistic tight-binding model. We plot Fermi energy E_F dependence of polarization angle θ at the local gate $V = 0$ eV and $V = 0.1$ eV in Fig. 2 (c) and (d). The polarization angles θ for the modes I (red lines) and III (green lines) behave similarly to each other, while that of the mode II (blue lines) reveals a completely different characteristics. This is a clear evidence that the modes I and III are connected to each other, forming a non-chiral edge mode, while the mode II can be identified as the non-trivial CEM. In Fig. 2 (d), we notice an abrupt change of polarization angle θ for the modes I and II when E_F is between 0 meV and 20 meV. Compared with the energy dispersion in Fig. 2 (b), we find that this change results from the strong hybridization effect between the modes I and II. Thus, the CEM and non-chiral mode are not well defined in this regime. In the other regime, we find a smooth change of SPs with respect to local gate voltages and chemical potentials.

Experimental detection of edge spin polarization - Our theoretical calculations based on both the effective model and realistic tight-binding model have clearly demonstrate electrically tunable SP in magnetically doped $(\text{Bi,Sb})_2\text{Te}_3$. However, the experimental detection of SP is not an easy task since the bulk is FM and it is unclear how to distinguish SP of CEMs from that of bulk

ferromagnetism by magnetization measurement. In contrast, when the Fermi energy is tuned into the bulk gap, the transport signals are dominated by CEMs. Thus, it is more promising to search for SP of CEMs from transport measurements.

Our proposal is based on a four terminal device with a FM probe as the fourth probe, as shown in Fig. 3 (a). This experimental setup is similar to that in the study of disordered leads in the QH system and here FM leads play the role of disordered leads²³. When SP of the CEM is parallel to magnetization \mathbf{M} of the FM lead, it can flow into the lead, while when they are opposite, it will be scattered. We apply a voltage drop between the leads V_1 and V_3 ($V_1 = V$ and $V_3 = 0$) and also introduce a split gate, denoted as SG in the Fig.3 (a). Due to the split gate, there are two types of currents flowing from the lead V_2 to V_4 : the current i_1 , which goes through V_3 , and the current i_2 flowing directly from V_2 to V_4 . Based on the Landauer-Büttiker formula^{24,25}, the current i_1 to the lead V_4 shares the same chemical potential as $V_3 = 0$, while the current i_2 is determined by the chemical potential in the lead $V_2 = V_1 = V$. Importantly, we assume that chemical potentials of two currents i_1 and i_2 have not reached equilibrium when they enter the FM lead. This is determined by the inelastic scattering length, which is estimated as several μm for the QH case²⁶, and we expect a similar length scale in our case. Thus, the corresponding SPs are also expected to be different for these two currents. Since the scattering rate into the FM lead V_4 depends on the relative angle between the SP of CEMs and \mathbf{M} . We expect the transmissions of $V_2 \rightarrow V_4$ and $V_3 \rightarrow V_4$ also depend on \mathbf{M} of the FM lead. As a result, the chemical potential in V_4 will vary when rotating \mathbf{M} . This provides a detectable signal, which is similar to the spin valve effect¹⁶, in transport measurements and can be directly related to SP of CEMs. It should be emphasized that the split gate SG plays an essential role here. Without the split gate, all currents flowing into V_4 come from V_3 , and thus the corresponding chemical potential in V_4 must be equal to that of V_3 , independent of magnetization direction of the FM lead.

To formulate this idea, we assume that only p ($p < 1$) fraction of the net edge current i_0 can flow from V_2 to V_3 due to the split gate, as shown in Fig. 2 (a), so $i_1 = pi_0, i_2 = (1-p)i_0$. We further assume the q' (q) fraction of the current i_1 (i_2) has spin polarizing along \mathbf{M} . Since SP of CEMs depends on chemical potential, it is reasonable to assume $q \neq q'$. Therefore, the currents from V_2 (V_3) to V_4 are $q'i_1$ and qi_2 , respectively, as shown in Fig. 3 (a). The Hall conductance G_{24} can be derived based on Landauer-Büttiker formula¹³ as

$$G_{24} = \frac{I_1}{V_2 - V_4} = G_0 \frac{(1-p)q + pq'}{q'} \quad (3)$$

with the conductance quanta $G_0 = \frac{e^2}{h}$. From Eq. (3), one can see that when there is no split gate ($p = 1$), $G_{24} = G_0 = \frac{e^2}{h}$, which recovers the quantized Hall

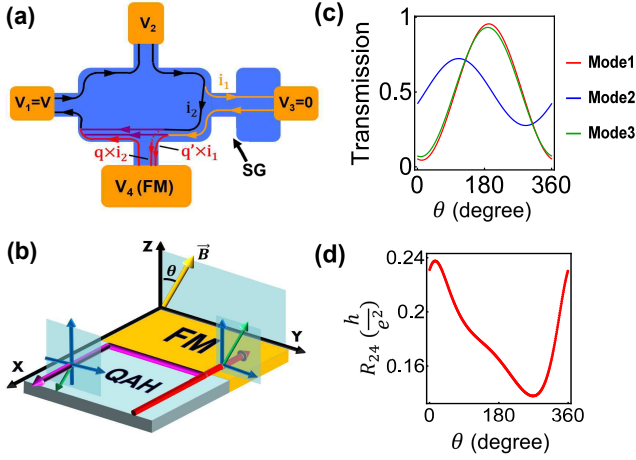


FIG. 3. Our proposed four terminal transport setup is shown in (a) with lines showing current flows. In (b), we show the spin valve effect at the FM lead V_4 : Only current with spin parallel to \mathbf{M} can flow into V_4 , while those with spin anti-parallel to \mathbf{M} will be reflected. θ dependence of transmission q_i s at $E_F = 33$ meV are plotted in (c). Based on this, we plot the evolution of transverse resistance R_{24} with θ in (d).

conductance and is independent of its spin information. When a split gate is introduced, $0 < p < 1$ and $q \neq q'$, and G_{24} will deviate from the quantized value and we discuss how to extract the information of SP of CEMs from the Hall resistance measurement in the Supplementary Materials¹³.

For the realistic systems of magnetically doped (Bi,Sb)₂Te₃, we have shown additional non-chiral modes coexisting with CEMs. Thus, it is natural to ask how these non-chiral modes influence the above transport measurement. We consider one pair of non-chiral edge mode (mode I and III in Fig. 2 (a)) and one CEM (mode II) and further assume no inter-channel scattering between different modes for simplicity. We take the modes I and II flowing clockwise (as shown in Fig. 3 (a)), and the mode III flowing counter-clockwise (flipping the directions of currents in Fig. 3 (a)). $q_{1,2,3}$ ($q'_{1,2,3}$) is defined as the transmission into FM probe of edge current i_2 (i_1) for the modes I,II and III, with $Q = q_1 + q_2$, $Q' = q'_1 + q'_2$ and $\bar{p} = 1 - p$. The explicit expression of transverse resistance is shown in the Supplementary Materials¹³. In the limit where the split gate vanishes ($p = 1 - \bar{p} = 1$), the transverse conductance G_{24} becomes

$$G_{24} = \frac{e^2}{h} \frac{7(Q' + q_3) - 3q_3Q'}{2Q' - q_3} \quad (4)$$

which deviates from the quantized value. Thus, in contrast to the single CME case, Hall resistance will depend

on the magnetization direction of FM leads even without any split gate for the case with both CME and non-chiral modes.

To apply Eq. (4) to magnetically doped Sb₂Te₃ films, we need to extract the coefficients q_i s from our realistic tight-binding model. As discussed above, q_i s are determined by the projection of SP of CEMs into the magnetization direction \mathbf{M} of FM leads. Since SP of CEMs only exists in the y - z plane, we only concern the projection of SP into the y - z plane. Let's assume \mathbf{M} has an angle θ relative to $+z$ direction in the y - z plane, as shown in Fig. 3 (b). The corresponding projection operator for CEMs is defined as:

$$P_\theta^{\uparrow\uparrow} = |\uparrow_\theta\rangle\langle\uparrow_\theta|, \text{ with } |\uparrow_\theta\rangle = e^{-i\sigma_x \frac{\theta}{2}} |\uparrow_z\rangle \quad (5)$$

Consequently, the angle dependent transmission $q_i(\theta)$ for the i th edge mode is given by

$$q_i(\theta) = \frac{\langle\psi_i|P_\theta^{\uparrow\uparrow}|\psi_i\rangle}{\langle\psi_i|P_\theta^{\uparrow\uparrow}|\psi_i\rangle + \langle\psi_i|P_\theta^{\downarrow\downarrow}|\psi_i\rangle} \quad (6)$$

where $|\psi_i\rangle$ is the wave function for the mode i . With Eq. 4 and Eq. 6, we can calculate the transmissions $q_i(\theta)$ s for the modes I, II and III as a function of θ and Fermi energy for the local gate voltage $V = 0.1eV$ for our realistic tight-binding model¹³. For the chemical potential $E_F = 33$ meV, θ dependence of transmission q_i s and the Hall resistance R_{24} , are shown in Fig. 3 (c) and (d), respectively. R_{24} shows a strong dependence on θ , thus revealing the spin valve effect for CEMs¹⁶. This provides a very clear and experimentally feasible evidence to detect spin signal in a QAH insulator.

Discussions - In summary, we have shown that SP of CEMs can be generated, manipulated and detected in a QAH insulator in a fully electric manner. This paves the way of potential applications for the QAH effect in spintronics. Disorder is inevitable in realistic samples and we show the stability of SP of CEMs against disorder in the Supplementary Materials¹³. Although we focus on the magnetically doped (Bi,Sb)₂Te₃ films here, the electric controllability of SP of CEMs is a general property of a QAH insulator. The bulk topology (non-zero Chern number) only guarantees the existence of CEMs, but the detailed form of wave functions of CEMs depends on local electric environment, and thus can be controlled by a local gate voltage. We expect a similar effect also occurs in other QAH insulators, such as Mn doped HgTe quantum wells³ and InAs/GaSb quantum wells²⁷, where the local gate voltage can induce a local Rashba spin-orbit coupling and tilt SP of CEMs.

Acknowledgement - We would like to acknowledge Cui-Zu Chang, Moses Chan, Abhinav Kandal, Jainendra Jain, Jagadeesh Moodera, Xiao-Liang Qi and Nitin Samarth for the helpful discussions.

-
- * cxl56@psu.edu
- ¹ K. v. Klitzing, G. Dorda, and M. Pepper, *Physical Review Letters* **45**, 494 (1980).
 - ² F. D. M. Haldane, *Physical Review Letters* **61**, 2015 (1988).
 - ³ C.-X. Liu, X.-L. Qi, X. Dai, Z. Fang, and S.-C. Zhang, *Physical review letters* **101**, 146802 (2008).
 - ⁴ R. Yu, W. Zhang, H.-J. Zhang, S.-C. Zhang, X. Dai, and Z. Fang, *Science* **329**, 61 (2010).
 - ⁵ C.-Z. Chang, J. Zhang, X. Feng, J. Shen, Z. Zhang, M. Guo, K. Li, Y. Ou, P. Wei, L.-L. Wang, *et al.*, *Science* **340**, 167 (2013).
 - ⁶ X. Kou, S.-T. Guo, Y. Fan, L. Pan, M. Lang, Y. Jiang, Q. Shao, T. Nie, K. Murata, J. Tang, *et al.*, *Physical review letters* **113**, 137201 (2014).
 - ⁷ J. Checkelsky, R. Yoshimi, A. Tsukazaki, K. Takahashi, Y. Kozuka, J. Falson, M. Kawasaki, and Y. Tokura, *Nature Physics* **10**, 731 (2014).
 - ⁸ A. Bestwick, E. Fox, X. Kou, L. Pan, K. L. Wang, and D. Goldhaber-Gordon, *Physical review letters* **114**, 187201 (2015).
 - ⁹ C.-Z. Chang, W. Zhao, D. Y. Kim, H. Zhang, B. A. Assaf, D. Heiman, S.-C. Zhang, C. Liu, M. H. Chan, and J. S. Moodera, *Nature materials* **14**, 473 (2015).
 - ¹⁰ X. Kou, L. Pan, J. Wang, Y. Fan, E. S. Choi, W.-L. Lee, T. Nie, K. Murata, Q. Shao, S.-C. Zhang, *et al.*, *arXiv preprint arXiv:1503.04150* (2015).
 - ¹¹ X. Zhang and S.-C. Zhang, in *SPIE Defense, Security, and Sensing* (International Society for Optics and Photonics, 2012) pp. 837309–837309.
 - ¹² J. Wu, J. Liu, and X.-J. Liu, *Physical review letters* **113**, 136403 (2014).
 - ¹³ See Supplementary Materials for details.
 - ¹⁴ N. Marzari and D. Vanderbilt, *Physical review B* **56**, 12847 (1997).
 - ¹⁵ I. Souza, N. Marzari, and D. Vanderbilt, *Physical Review B* **65**, 035109 (2001).
 - ¹⁶ B. Dieny, *Journal of Magnetism and Magnetic Materials* **136**, 335 (1994).
 - ¹⁷ C.-X. Liu, X.-L. Qi, H. Zhang, X. Dai, Z. Fang, and S.-C. Zhang, *Physical Review B* **82**, 045122 (2010).
 - ¹⁸ L. Fu, *Physical review letters* **103**, 266801 (2009).
 - ¹⁹ M. L. Sancho, J. L. Sancho, and J. Rubio, *Journal of Physics F: Metal Physics* **14**, 1205 (1984).
 - ²⁰ M. L. Sancho, J. L. Sancho, J. L. Sancho, and J. Rubio, *Journal of Physics F: Metal Physics* **15**, 851 (1985).
 - ²¹ J. Wang, B. Lian, H. Zhang, and S.-C. Zhang, *Physical review letters* **111**, 086803 (2013).
 - ²² J. Wang, B. Lian, H. Zhang, Y. Xu, and S.-C. Zhang, *Physical review letters* **111**, 136801 (2013).
 - ²³ S. Datta, *Electronic transport in mesoscopic systems* (Cambridge university press, 1997).
 - ²⁴ M. Büttiker, *Physical Review Letters* **57**, 1761 (1986).
 - ²⁵ M. Büttiker, *Physical Review B* **38**, 9375 (1988).
 - ²⁶ S. Koch, R. Haug, K. v. Klitzing, and K. Ploog, *Physical review letters* **67**, 883 (1991).
 - ²⁷ Q.-Z. Wang, X. Liu, H.-J. Zhang, N. Samarth, S.-C. Zhang, and C.-X. Liu, *Physical review letters* **113**, 147201 (2014).